Theoretical study of oxygen-deficient $SnO_2(110)$ surfaces

Matti A. Mäki-Jaskari* and Tapio T. Rantala†
Institute of Physics, Tampere University of Technology, P.O. Box 692, FIN-33101 Tampere, Finland
(Received 4 December 2001; revised manuscript received 6 March 2002; published 24 June 2002)

Theoretical consideration of recently proposed ordered stoichiometric and oxygen-deficient (110) surfaces of SnO_2 crystal with 1×1, 1×2, 2×1, and 1×4 symmetries have been done. We use a first-principles density-functional method and plane-wave basis, combined with pseudopotentials to calculate surface electronic structures, surface geometries, and energetics. Calculated surface formation energies suggest that stability of the oxygen-deficient surfaces decrease with increasing oxygen deficiency. At oxygen-deficient 1×2 and 1×4 surfaces tin atoms similar to those in SnO crystal were found to appear. In all cases, the highest occupied orbitals were considerably localized at the sites of surface oxygen vacancies. The 2×1 added row surface structures were found to be relatively stable and associated with the decrease of the band gap due to jagged surface. Also, ultraviolet optical absorption coefficients for different surface structures were determined by using the electric dipole approximation with a scissor correction.

DOI: 10.1103/PhysRevB.65.245428 PACS number(s): 68.35.−p, 73.20.−r, 78.68.+m

I. INTRODUCTION

Recently, progress in the study of ordered metal oxide surfaces including SnO_x surfaces have been reported in literature.[1–4] To ascertain the results, theoretical considerations are needed, offering also an opportunity to connect theoretical studies to other metal oxide surface systems with related structures. Among metal oxide compounds with rutile structure, tin oxide as not being a transition metal is particularly suitable from a theoretical point of view.[2] Its various surface structures are, however, not well known.[2]

In theoretical studies of the electronic structure of oxygen-rich ($x\geqslant2$) and oxygen-deficient ($x<2$) tin dioxide surfaces,[5–9] usually the so-called stoichiometric ($x=2$) and reduced surfaces are considered (shown in Fig. 1). To simplify, most significant features are associated with oxygens, which acting as O^{2-} ions, have occupied *p* related states near the top of the valence band. In the case of stoichiometric surface, *p* states of surface oxygens largely contribute to the valence-band maximum. Tin atoms can alter their ionic role from Sn^{4+} to Sn^{2+} at oxygen-deficient surfaces ($x<2$) causing a type of occupied ''dangling bonds.''

Here we will consider examples, motivated by recent results of semiconductor research of other SnO_2 surfaces with surface stoichiometry $x\leqslant2$. In case of these ''oxygen-deficient'' (110) surfaces, recent atomic resolution microscopy measurements show that the surface can be composed of domains with 1×1, 1×2, 2×1, and 1×4 symmetries.

In experimental arrangements these surfaces have typically been produced by applying thermal annealing in vacuum after sputtering treatments,[2,10,11] though other techniques exist.[12,13] In service at normal conditions, formation of oxygen-deficient metal oxide surfaces can also be associated with oxidation reactions at the surface and diffusion of oxygen vacancies or tin atoms to the surface. Of particular importance has been the catalytic oxidation of carbon monoxide to carbon dioxide and oxidation of methane at tin oxide surface. Based on applied surface preparation and measurement techniques, surface oxygen deficiency associated to in-plane oxygen vacancies is assumed to be important in catalyzing dissociation of water.[14]

The (110) surface of tin oxide is the most common of the faces of rutile structure tin oxide.[1] However, there is also interest in other ordered tin dioxide surfaces associated, for instance, with tin oxide wires[15] and on anatase structures of tin oxide.[16] In these cases, the proposed results for oxygen-deficient (110) surfaces can be qualitatively adapted.

Earlier, we studied the reduced and stoichiometric (110) surfaces of SnO_2 (Ref. 9) focusing mainly on the surface geometry, charge distribution, band structure, and optical properties. These properties that are here further considered, entail connections to electronic spectroscopies.[1,2]

The paper is organized as follows. In Sec. II the calculation method and its applicability is described following with consideration of surface energetics and geometries in Sec. III. In Sec. IV discussion of surface electronic structure together with a brief discussion of optical absorption is presented. Finally, in Sec. V conclusions are drawn from the results.

II. METHOD

The computational first-principles density-functional approach applied here is based on the plane-wave basis set and pseudopotential concept to describe electron-ion interaction (CASTEP/CETEP code),[17] briefly discussed also in Ref. 9. Utilizing ultrasoft pseudopotentials[18] (USP) the plane-wave basis set can be limited considerably still with good accuracy in bulk and surface geometries.[9] Oxygen atoms are described by six valence electrons and tin atoms by four plus the corresponding pseudopotential ion cores. As will be indicated separately, a few calculations were reproduced by using a more accurate nonoptimized norm-conserving pseudopotentials (PSP).[19] This pseudopotential includes in addition to the four valence electrons of Sn, the 18 electrons of the *N* shell.

The electronic interactions were in all cases taken into account with generalized-gradient approximation (GGA).[20] Ground state of the electronic systems were obtained by density mixing scheme, in which the sum of electronic eigenvalues is minimized. In the case of oxygen molecules, spin po-

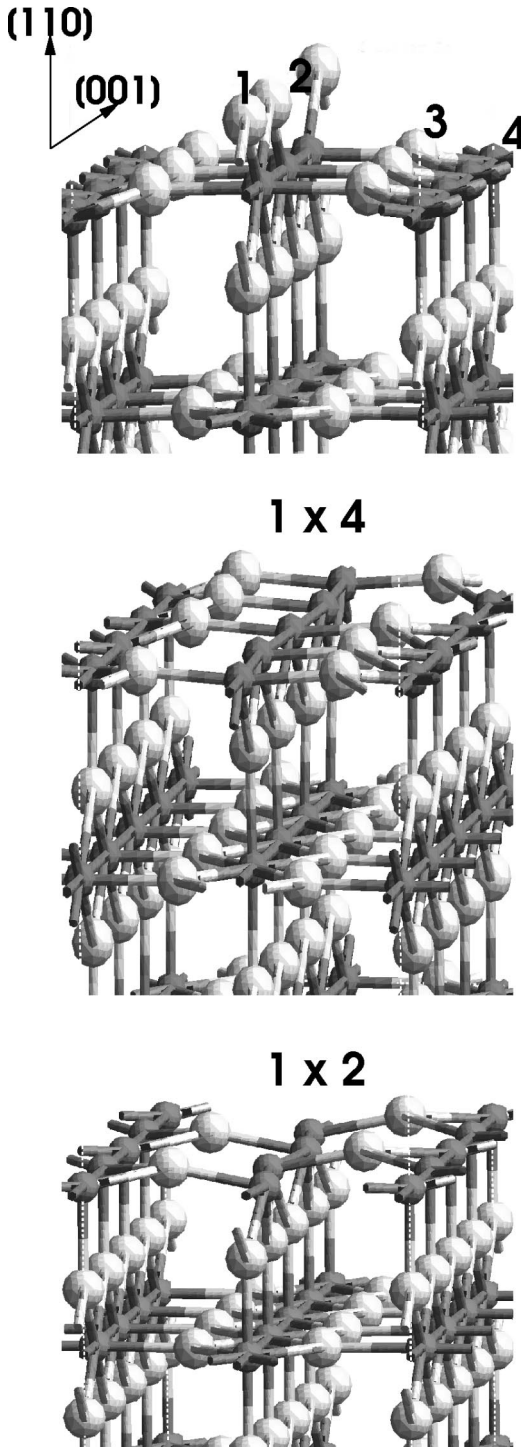

FIG. 1. Relaxed SnO_2 (110) surface geometries corresponding to bridging vacancy model (top) and 1×4 (middle) and 1×2 (below) surface vacancy models. Bridging oxygen is indicated by label 1, bridging oxygen vacancy by 2, in-plane oxygen by threefold and fivefold coordinated surface tin by label 4. With all bridging oxygen atoms present the surface is called stoichiometric. If all bridging oxygens are removed, the so-called reduced surface is formed. The illustrated surface unit cell of the 1×2 surface is doubled along the (001) direction.

larization was taken into account. As expected for nontransition metal oxides, spin polarization was not found to decrease total energies in other cases.[1] To sample Brillouin zone, the number of symmetrized Monkhorst-Pack k points[21] was 6 for the smallest systems. The plane-wave cutoff was 400 eV.

With USP, total energies (which are here identified to chemical potentials) were -977.15 eV for a bulk SnO_2 unit, -97.9 eV for an atom of bulk white tin and -873.0 eV for O_2 molecule. The heat of formation of bulk SnO_2 rutile structure crystal was slightly overestimated to be 6.2 eV, in comparison with the experimental value of 6.02 eV (at 298 K).[22] For bulk SnO litharge structure crystal, the heat of formation 3.1 eV is obtained in comparison with experimental value of 3.0 eV.[22] All calculations were performed for charge neutral systems at zero temperature and pressure conditions.

To investigate electronic structures, total density of states (DOS) were evaluated together with partial charge contributions to the DOS. This provides an idea of structurally derived differencies in chemical and optical properties. Mulliken population analysis was also performed, in which Mulliken charges of atoms and bond populations of pairs are calculated in terms of density matrix and overlap matrix.[23] These are obtained from projections of the one-electron eigenfunctions to the atomic orbitals.

For oxygen-deficient structures ultraviolet optical dielectric function calculations with light normal to surface were performed similarly as in Ref. 9. Calculations of dipole transition matrix elements were carried out in the reciprocal space with a correction term due to the nonlocality of the pseudopotential[24] included. The use of the local density and GGA approximations are known to underestimate excited-state energies. This is corrected by using the scissor operation that shifts rigidly the unoccupied energy levels by 2.25 eV to reinstate experimentally known direct bulk band gap (E_g) of SnO_2.[9] Here the the band gap was chosen to be $E_g = 3.6$ eV.[25] Some doubts about the applicability of ultrasoft pseudopotential approximation in these circumstances exist, due to use of pseudizated wave function for valence electrons.[26] However, our comparison indicates relatively small correction with respect to PSP at low transition energies that are of interest here.[9]

III. ENERGIES AND GEOMETRIES OF (110) SURFACES

Three SnO_2 (110) surfaces containing oxygen vacancies are illustrated in Fig. 1, ordered with increasing oxygen deficiency in going downwards. A well-known bridging oxygen vacancy surface (shown in Fig. 1) is expected to form from reduced or oxidized surface most easily. In connection with the surfaces annealed at elevated temperatures, the reduced surface with 1×1 surface symmetry is expected to be formed at the temperature of the order of 700 K in vacuum annealing conditions from the stoichiometric surface with 1×1 surface symmetry.[27] At higher temperature conditions, two models of 1×2 and 2×1 symmetry[10,11,28] have been proposed (also known as zigzag row and cross linked added row models). Corresponding geometries are illustrated in

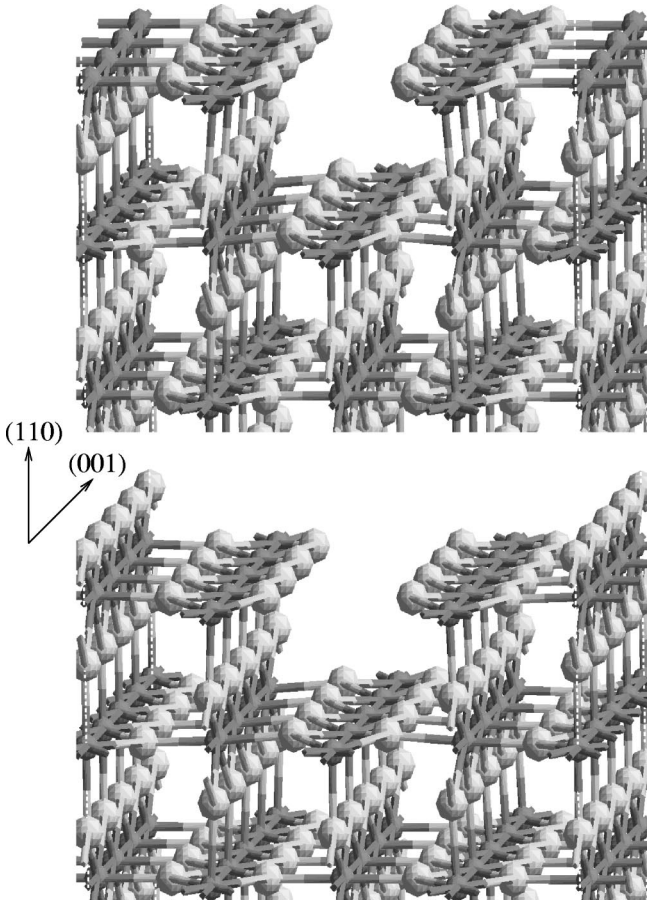

FIG. 2. Relaxed SnO_2 surface geometries of 2×1 surface structures, corresponding to oxygen-deficient (top) and stoichiometric (below) surfaces. The illustrated surface unit cells are quadruplicated along (001) direction.

Fig. 1 (below) and in Fig. 2 (above). At elevated temperature conditions the formation of 2×1 structure can be associated with the formation of special step edges.[29] Also, in the case of TiO_2 surfaces with the presence of excess oxygen, growth of surfaces related to this model can be favorable.[30] A model for lower temperature annealed (600–1000 K) oxygen-deficient surface with 1×4 symmetry[10] is illustrated in Fig. 1 (middle).

As idealized models to study these surfaces, corresponding periodic $Sn_{40}O_{68}$, $Sn_{20}O_{32}$, and $Sn_{26}O_{50}$ slabs with symmetry 1×4, 1×2 and 2×1 were constructed. For the reduced 1×1 surface the slab composition was $Sn_{14}O_{26}$. To compare the surfaces with a bridging oxygen vacancy surface, also two slabs with compositions $Sn_{18}O_{34}$ and $Sn_{40}O_{78}$ were constructed. With one bridging oxygen removed from both sides of the stoichiometric slabs, these surfaces correspond to 1×3 and 1×4 surface symmetries. For all systems geometry optimization was performed with the atomic plane at the center remaining fixed to correspond bulk geometry.[9] The slabs were made mirror symmetric along [110] direction and the vacuum thickness was about 10 Å.

Energies with modest differencies around 3.0 eV were calculated for vacancy formation energies E_v, which were evaluated from $E_v=\frac{1}{2}(E_{sl}+nE_{O_2}-E_{sto})/n$. In this equation E_{sl} are the total energies of the surface slabs, having n oxygen pairs removed from the corresponding stoichiometric slab that has a total energy of E_{sto}. For the 2×1 surface model, calculation of E_v is not feasible since also tin atoms are removed. The small differences between surface vacancy formation energies suggests that different oxygen-deficient surface reconstructions may easily coexist, unless surface is not uniformly conditioned at microscopic scale. Significantly larger vacancy formation energies were calculated in other cases where oxygen atoms were removed below or from the surface of a slab containing also bridging oxygens. These less oxygen-deficient surfaces have recently been investigated by using density-functional method,[7] and will be considered here only to compare with. Thus, it can be expected that surface geometries of Fig. 1 (or their local structures) are relevant, although the present study cannot rule out the existence of other more stable geometries at certain oxygen deficiency. Other possibilities for surfaces with low vacancy formation energies that may need to be mentioned can be associated with parallel rows of surface in-plane oxygen vacancies along [001] direction. In these surfaces one in-plane oxygen is removed from stoichiometric or alternatively from reduced 1×1 surface. For the case in which in-plane oxygen is removed from stoichiometric surface, vacancy formation energy of 3.0 eV was obtained. Formation of this surface model can compete with formation of reduced surface, which have same surface composition.[7] In the second case, in which one in-plane oxygen was removed from reduced surface, lowest vacancy formation energy of 2.5 eV was calculated. Therefore this model may provide an alternative for the most oxygen-deficient 1×2 surface.

To examine in more general terms surface energetics, also a comparison between total energies of surface models and corresponding bulk and gas phase systems was performed. This study is related to those presented in references[31–33] for thermodynamics of GaAs and TiO_2 surfaces. Surface energy E_s of a slab with total energy E_{sl} and surface area A is $E_s=(E_{sl}-N_{Sn}\mu_{Sn}-N_O\mu_O)/2A$, where N_O and N_{Sn} are numbers of oxygen and tin atoms in the slab. The sum of chemical potentials of tin μ_{Sn} and oxygen μ_O atoms, $\mu_{Sn}+2\mu_O$, is equal to the chemical potential μ_{SnO2} of bulk SnO_2, due to the presence of bulk phase. The values of μ_{Sn} and μ_O are yet unknown. Then, surface energy becomes $E_s=[E_{sl}-N_{Sn}\mu_{SnO2}+(2N_{Sn}-N_O)\mu_O]/2A$, where the last term is chemical potential of removed oxygens. The chemical potential for oxygen is approximated by using half of the chemical potential of the free oxygen molecule. Almost independently of the applied chemical potential the ordering of the surface energies is

$$E_{\text{Stoich}}<E_{\text{Br.vac}}<E_{2\times1}<E_{\text{Reduc}}<E_{1\times4}<E_{1\times2},$$

increasing from 1.3 J/m^2 of stoichiometric model to 5.9 J/m^2 of 1×2 surface model (shown in Fig. 3). The surface energy increases with increasing surface oxygen deficiency, which is obvious also from the minor differencies of the vacancy formation energies.

The above assumptions about surface energetics for differing surfaces requires further consideration in few respects.

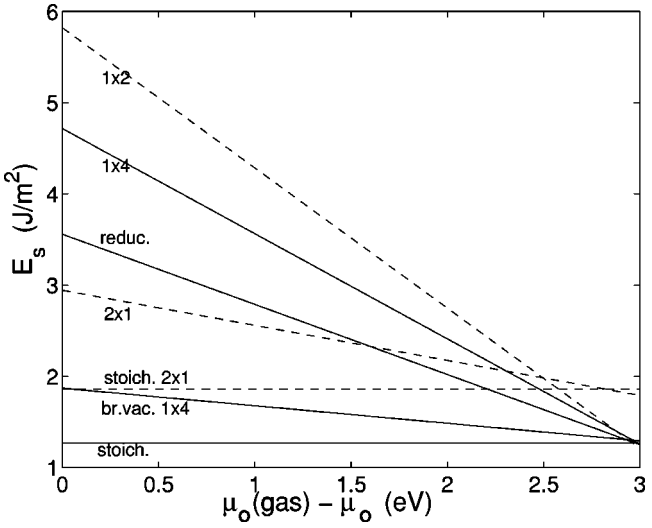

FIG. 3. Surface energies E_s for the surface structures as a function of chemical potential of oxygen atom μ_O (see text). The sum $\mu_{Sn}+2\mu_O$ is equal to chemical potential of bulk SnO_2 and at the left side μ_O equals potential of oxygen atom in free oxygen molecule $\mu_O(gas)$. The Stoich. 2×1 and 2×1 surfaces correspond to the surfaces illustrated of Fig. 2 below and above, respectively.

First, at elevated temperatures various temperature-dependent contributions are expected to be largely canceled when E_v and E_s are evaluated. The differencies in the contribution of configurational part of the entropy[34,35] are expected to be relatively insignificant in comparison to surface energy differencies. Second, surface energies E_s as a function of μ_O are different as illustrated in Fig. 3. The left side of the graph corresponds to the above-mentioned limit for μ_O, where oxygen gas is in equilibrium with bulk and surface. At the right-side limit, the chemical potential for tin equals the chemical potential of bulk tin. This limit is unrealistic in many known cases, since otherwise, based on thermodynamics, bulk Sn phase may separate from bulk SnO_2. If the total energies of the oxygen-deficient surface slabs are compared with independent bulk Sn (or SnO) and bulk SnO_2 crystal phases, it was noticed that the slab systems are less stable. Therefore, it can be claimed that there can be an oxygen-deficient two-phase bulk system that is more stable than oxygen-deficient surface.

One of the most striking result of the above surface energy comparison is the stability of the surface with 2×1 symmetry. It may thus be questioned what is the stability of this surface when bridging oxygens are included. Such a surface geometry, which we shall term as stoichiometric 2×1 surface, is illustrated in Fig. 2 below. As shown in Fig. 3 this surface has a slightly larger surface energy than the stoichiometric surface. In addition to the above two 2×1 surface models, for TiO_2 also an another more complicated geometry, named as Ti_2O_3 added row, has been proposed[36–38] (not shown here). For such a surface slab ($Sn_{24}O_{46}$) a surface energy of value 3.0 J/m^2 was calculated, which is close to that of the 2×1 model. However, in the case of tin oxide, this geometry is not identified and thus the 2×1 geometries of Fig. 2 are here considered.

The relaxations of the surface atoms of the different surface models were quite similar. All surface oxygens relax outwards (along [110]) with respect to their surrounding surface tin atoms, except in the case of the reduced surface. In this case, the outward relaxation of the fourfold coordinated surface tin atom (Sn^{2+}) is slightly more pronounced. All threefold coordinated surface tin atoms relax about 0.15 Å toward the nearest oxygen vacancy. The differencies of surface relaxations in comparison to stoichiometric surface are largest in the case of the 1×2 surface. Its surface in-plane oxygens are displaced 0.25 Å toward nearest three-fold coordinated surface tin atoms, and outward (along [110]) similarly with stoichiometric surface. The threefold coordinated surface tin atoms relax also inward 0.15 Å with respect to tin atoms at the corner of the surface unit cell. In the case of 1×4 surface, three-fold coordinated tins with their nearest in-plane oxygens are displaced about 0.15 Å toward the surface vacancy, which are the most prominent displacements of this surface with respect to the stoichiometric surface.

IV. SURFACE ELECTRONIC STRUCTURE

The electronic structures of the different surfaces seems to share many common features. The valence band of SnO_2 is known to be divided into the upper valence band, mainly of oxygen *p* type and to lower oxygen *s* type band.[1] The oxygen *p*-type states contribute the valence density of state maxima, as illustrated in Fig. 4. The highest energy level of both type of bands consist of occupied surface states whose density originates in addition to the surface atoms also slightly from first sublayer oxygens. At the position of the surface oxygens surface states are significantly contributed by oxygen ''dumb bells'' pointing out to vacuum. Decrease of the Madelung field at surfaces plays an important role in ''destabilizing'' surface O^{2-} and Sn^{4+} ions with respect to corresponding bulk ones.[1,39] The decrease of the Madelung field is expected to become more effective as surface oxygen ions are removed. In all of the surface models here considered, lowest energy conduction-band energy states are also surface states.

Considering surface tin atoms, significantly different contributions depending largely on differing coordination and ionic charge occurs. With decreasing coordination from fivefold coordinated Sn surface ions to the threefold (approximately sp^2) coordinated surface tin atoms of 1×4 and 1×2 surfaces, Mulliken valence charges increases from a value of about 2.5 to over 3 electrons. Consequently, the threefold coordinated surface tin atoms have a large Sn-*p* type of contribution. Qualitatively, the increase of charges of tin ions can be explained in terms of Pauling's bond strength[40,41] and charge compensation of surface ions to avoid electrostatic instability.[42] Some changes of surface bonding are also present. In the case of bridging oxygen atoms, associated Sn-O bond length is contracted 0.07 Å from the corresponding bulk value. This bond has the largest bond population and the sixfold coordinated Sn atom has significantly larger Mulliken charge with respect to the tin atoms below surface layer. At 1×4 and 1×2 surfaces, the threefold coordinated tin ions bind more strongly to the nearby surface in-plane oxygen atom according to the bond

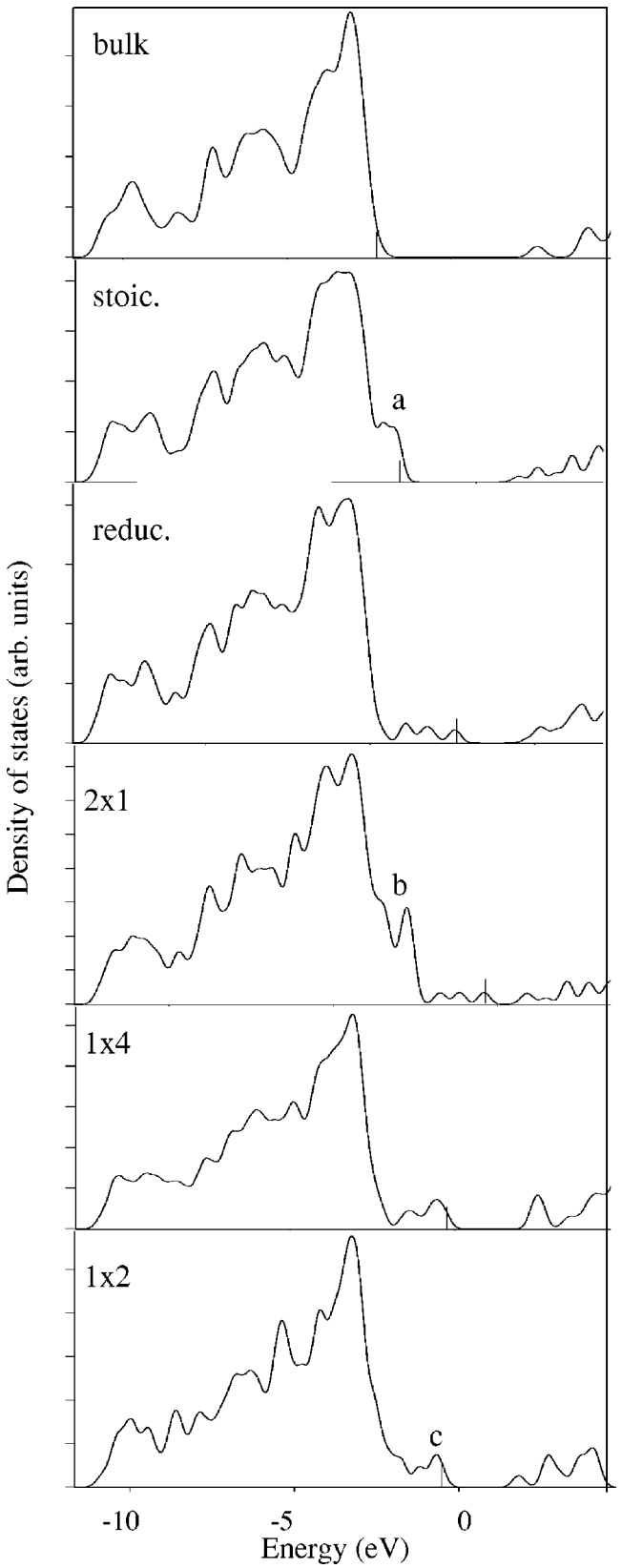

FIG. 4. Total density of states of the upper valence band of the considered slab models. The line indicates the highest occupied state. The largest density maxima are attributed mainly to oxygen *p* orbitals. The DOS maxima labeled by *a* and *b* are due to the surface bridging oxygen *p* orbitals. The DOS maximum labeled by *c* corresponds to the distribution of 1×2 model shown in Fig. 5.

population analysis. More generally, the coordination and local geometry of fourfold and, more significantly, threefold coordinated surface tin atoms have similarity with tin monoxide and with some other Sn(II) compounds. In these cases, part of the charge of broken Sn-O bonds of the crystal systems are in a form of ''hats'' covering tin atoms (also known as lone pair hats) and located in the space of removed bond.[43–45] Character of such a charge distribution is associated with a state density close to the Fermi level with a considerable Sn-5*p* type of contribution. A closely related charge distribution is present also in the case of oxygen deficient (110) surfaces that will be illustrated in more detail.

Some chemical differences between surface models are obvious from the different DOS curves for bulk, stoichiometric, reduced and 2×1, 1×4, and 1×2 models shown in Fig. 4. Characteristic surface-state features attributed to bridging oxygen O-*p* dumb bells are indicated by label *a* in Fig. 4. The corresponding orbitals in space are shown in Fig. 5. The removal of a bridging oxygen from the row of bridging oxygens (i.e., bridging oxygen vacancy model) changes DOS by forming a peak above the top of the valence band in the stoichiometric model[7] (not shown here). The charge of the associated highest occupied orbital is most significant at the position of the removed oxygen. As discussed in Refs. 5 and 6 and 9, and shown in Figs. 4 and 5, removal of all bridging oxygens, cause surface states high in the bulk band gap associated to fourfold Sn^{2+} ions, with in-plane oxygen *p* contribution. The 2×1 surface model has similar tin Sn^{2+} with lower density, and thus, similar surface DOS features as shown in Fig. 4. This model also contains twofold coordinated surface oxygens that have similarity with bridging oxygens and contribute a similar DOS feature labeled by *b* in Fig. 4. In case of the 1×2 model, surface states, with the charge hats as discussed above, are clearly formed as shown in Fig. 5. The corresponding maxima in DOS are labeled by *c* in Fig. 4. At lower energy states (below 1 eV from the top of the valence band) charge hats overlap significantly with nearby fourfold surface tins in a way that charge becomes smeared over empty in-plane vacancy site (not shown here). This overlap obviously has a stabilizing effect. The charge distribution of 1×4 surface has a qualitative similarity with reduced and 1×2 models. In the case of a less stable surface vacancy model, in which in-plane oxygen is absent from stoichiometric surface, highest occupied orbital were significantly localized to the position of removed oxygen atom.

Concerning the differences between USP and PSP pseudopotential results, a difference in charge density in a close vicinity of surface Sn ions was observed.[9] As indicated by label *B* in Fig. 5, in the case of PSP, additional localized charge appear at surface Sn sites of both stoichiometric and nonstoichiometric models in comparison to the case of USP. The surface tin atoms, at the center of the surface unit cell, also have highest Sn-4*s*, Sn-4*p*, and Sn-4*d* electron energies in the cases of stoichiometric, reduced and 1×2 surface models. A simple explanation for this result is the largest valence charge of these tin atoms in comparison with other tin atoms in the unit cells.[46]

Also, parts of DOS above the conduction-band minima are shown in Fig. 4. Corresponding lowest occupied orbitals

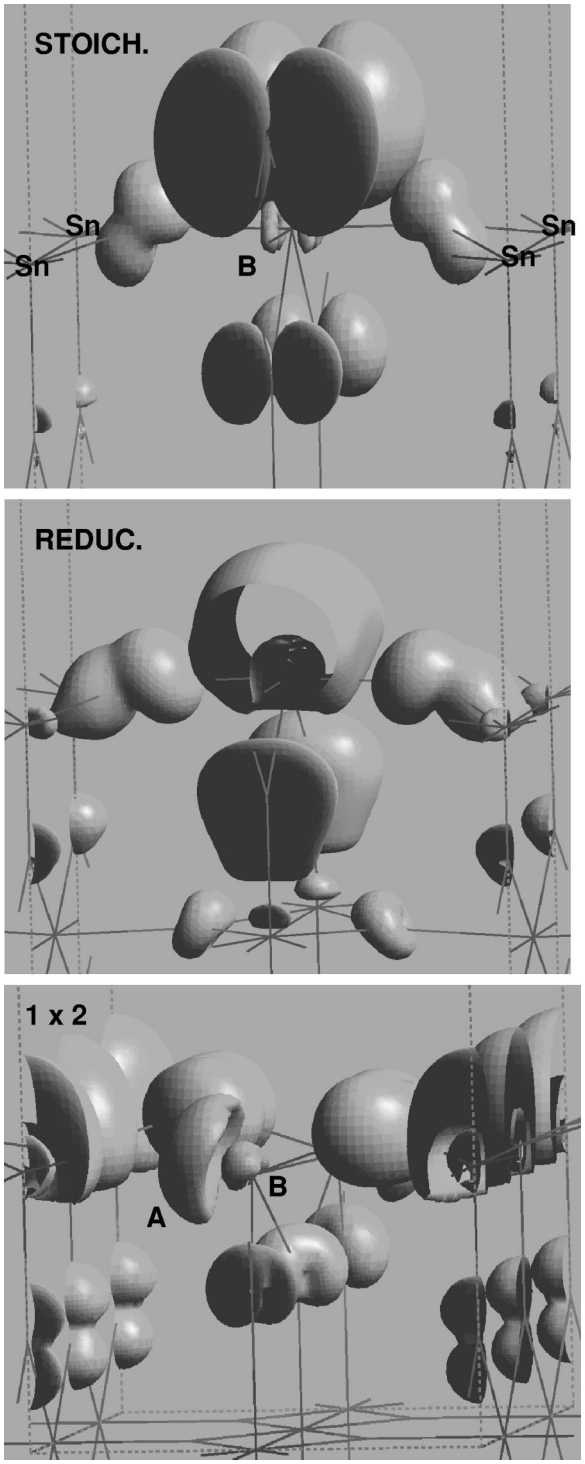

FIG. 5. Highest occupied orbitals integrated over the first Brillouin zone of stoichiometric, reduced and 1×2 surface models calculated by using PSP pseudopotential. The label *A* indicates tin ''charge hat.'' Label *B* shows charge distribution absent in the case of USP pseudopotential. These isocharge surfaces corresponds to the charge density of about 0.01 e/Å^3.

for stoichiometric and reduced models are shown in Fig. 6. In the case of stoichiometric model, separation between valence- and conduction-band energy levels is decreased with respect to bulk. The separation is further decreased in

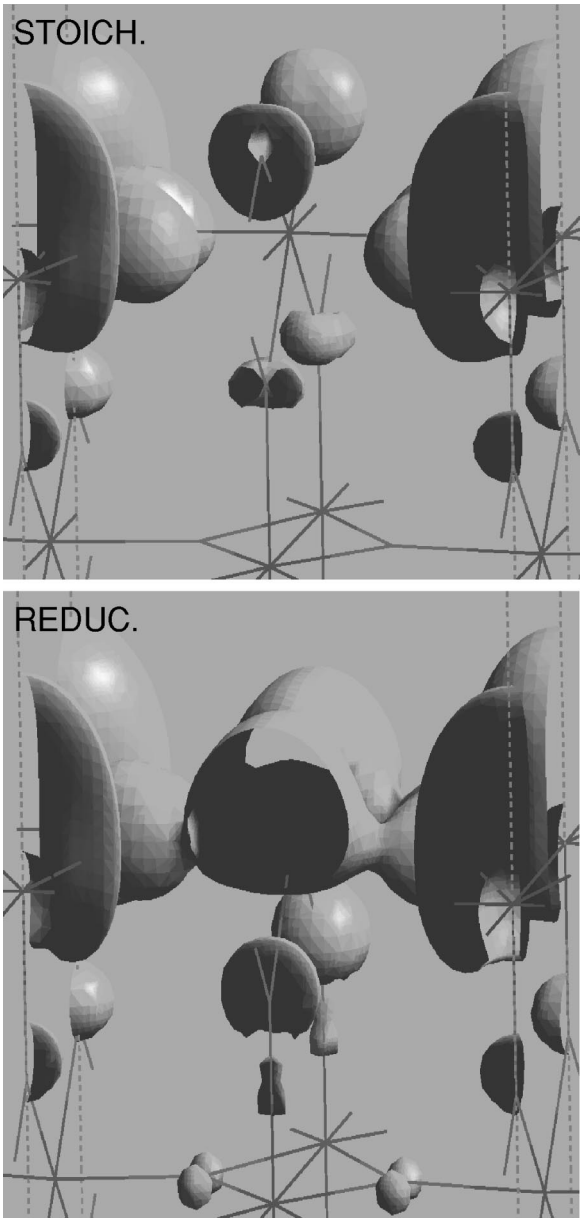

FIG. 6. Distribution of lowest unoccupied orbitals of stoichiometric (top) and reduced surface models (bottom) calculated by using USP pseudopotential. Significant localization is observed at the site of the fivefold coordinated surface tin atom.

case of oxygen-deficient surfaces. This is in agreement with experiments with oxygen-deficient SnO_2 surfaces.[47] Most considerable decrease of separation between valence- and conduction-band energy levels is observed in the case of the 2×1 model. The decrease of the energy-level separation can be seen as an indication of the decreased stability of the surface systems.[48] However, in the case of 2×1 surface this reasoning does not seem to apply. The explanation for the smallest separation between valence and conduction bands is that the valence and conduction band states (projected to surface atoms) are lower in energy at hollow area of the 2×1 surface. In agreement with experimental results of scanning tunneling microscopy, hollow area shows a dark contrast.[28] There are many effects that can result in stabili-

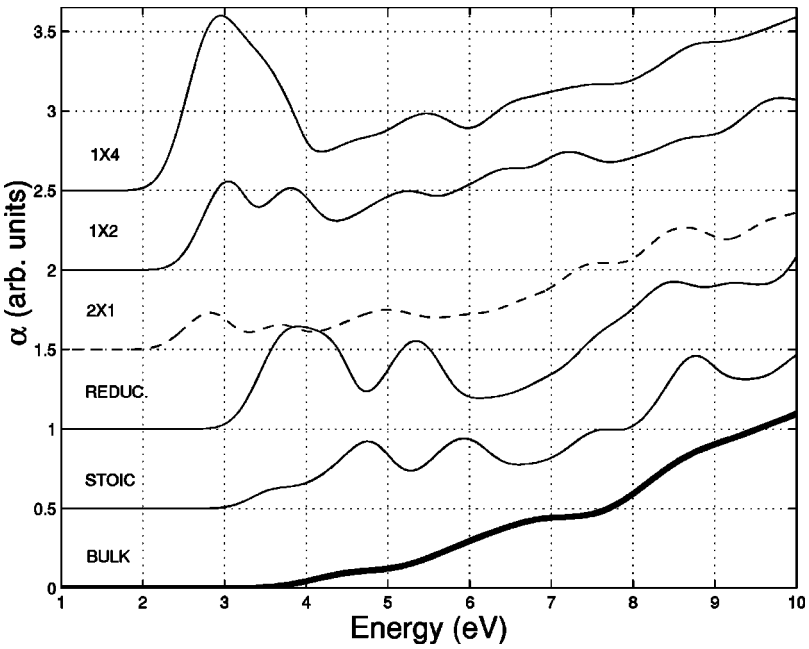

FIG. 7. Absorption coefficients for the surface systems as a function of excitation energy.

zation of the hollow sites including absence of least coordinated surface ions together with decreased repulsive interactions and larger Madelung field than at plane (110) surface. Actually, for oxygen atoms the energy levels at the hollow site were slightly (0.5 eV) below the energies of those oxygen atoms in the middle of the slab.

Earlier, a good agreement was found between calculated and experimental ultraviolet absorption at SnO_2 surface.[9] Here the applied electric dipole approximation predicts that ultraviolet optical absorption in transition energies below 4 eV is entirely contributed by surfaces, as shown in Fig. 7. All vacancy models cause about 1 eV decrease of the absorption edge with respect to stoichiometric and reduced surfaces. Thus, the presence of further surface oxygen deficiency and 2×1 type of surface geometry is observed to decrease ultraviolet absorption edge. The effects of incident light polarization were also checked. It was found that, except for the case of 2×1 surface, absorption is slightly more strong with the light polarized along $[1\bar{1}0]$ direction with as compared to [001] polarization.

V. CONCLUSIONS

Theoretical calculations confirm the existence of recently proposed 2×1, 1×4, and 1×2 surface vacancy structures of SnO_2 (110). Surface geometries are similar to the ones proposed earlier for titanium oxide. Atomic surface relaxations differ slightly from those of the stoichiometric surface, with in-plane oxygens relaxing outwards in all cases considered. Threefold coordinated surface tin atoms with their nearest in-plane oxygen atoms relax towards surface vacancy site. Nearly equal energies for surface vacancy formation (3.0 eV) were calculated for all structures. Consequently, surface energy of the considered surfaces increase with increasing oxygen deficiency. Reduced and oxidized 2×1 surfaces were found to be relatively stable. The observed differences between 1×2 and 1×4 structures were relatively modest.

The highest occupied orbital has a significant contribution at the site of the removed oxygen. In case of the 1×2 and 1×4 surfaces these orbitals have qualitative characteristics similar to those found in SnO crystals. Surface states were found in all studied cases, including also the stoichiometric surface, at the top of Sn ($4s$,$4p$,$4d$), O$2s$ and O$2p$ type of bands. The electronic structure of 2×1 model is associated with an additional microscopically nonhomogeneous band bending that decreases the observed band gap. Concerning ultraviolet optical absorption, in comparison with the previously published stoichiometric and reduced surface models, absorption edge is predicted to decrease about 1 eV in the cases of 2×1, 1×4, and 1×2 surfaces.

ACKNOWLEDGMENTS

We acknowledge the Academy of Finland for funding MECA project, within which this work has been carried out. We also acknowledge computational resources of the Center for Scientific Computing (CSC) Espoo, Finland.

*Email address: Matti.Maki-Jaskari@tut.fi
†Email address: Tapio.Rantala@tut.fi

[1] V. E. Henrich and P. A. Cox, *The Surface Science of Metal Oxides* (Cambridge University Press, Cambridge, England, 1994).
[2] D. P. Woodruff, *The Chemical Physics of Solid Surfaces, Oxide Surfaces* (Elsevier, New York, 2001).
[3] R. C. Smart and J. Nowotny, *Ceramic Interfaces Properties and Applications* (The Institute of Materials, University Press, 1998).
[4] P. A. Cox, *Transition Metal Oxides: An Introduction to Their Electronic Structure and Properties* (Clarendon, Oxford, 1992).
[5] I. Manassidis, J. Goniakowski, L. N. Kantorovich, and M. J. Gillan, Surf. Sci. **339**, 258 (1995).
[6] T. T. Rantala, T. S. Rantala, and V. Lantto, Mater. Sci. Semicond. Process. **3**, 103 (2000).

[7] J. Oviedo and M. J. Gillan, Surf. Sci. **467**, 35 (2000).
[8] J. Oviedo and M. J. Gillan, Surf. Sci. **463**, 93 (2000).
[9] M. A. Mäki-Jaskari and T. T. Rantala, Phys. Rev. B **64**, 075407 (2001).
[10] C. L. Pang, S. A. Haycock, H. Raza, P. J. Møller, and G. Thornton, Phys. Rev. B **62**, R7775 (2000).
[11] M. Sinner-Hettenbach, M. Göthelid, J. Weissenrieder, H. Schenck, T. Weiß , N. Barsan, and U. Weimar, Surf. Sci. **477**, 50 (2001).
[12] M. L. Knotek and P. J. Feibelman, Phys. Rev. Lett. **40**, 964 (1978).
[13] V. M. Bermudez, J. Vac. Sci. Technol. **20**, 51 (1982).
[14] V. A. Gercher and D. F. Cox, Surf. Sci. **312**, 106 (1994).
[15] Z. R. Dai, Z. W. Pan, and Z. L. Wang, Solid State Commun. **118**, 351 (2001).
[16] M. Lazzeri, A. Vittadini, and A. Selloni, Phys. Rev. B **63**, 155409 (2001).
[17] V. Milman, B. Winkler, J. A. White, C. J. Pickard, M. C. Payne, E. V. Akhmatskaya, and R. H. Nobes, Int. J. Quantum Chem. **77**, 895 (2000).
[18] D. Vanderbilt, Phys. Rev. B **41**, 7892 (1990).
[19] M. Teter, Phys. Rev. B **41**, 7892 (1993).
[20] J. P. Perdew and Y. Wang, Phys. Rev. B **46**, 6671 (1992).
[21] H. J. Monkhorst and J. D. Pack, Phys. Rev. B **13**, 5188 (1976).
[22] D. D. Wagman, W. H. Evans, V. B. Parker, R. H. Schumm, I. Halow, S. M. Bailey, K. L. Churney, and R. L. Nuttall, *The NBS Tales of Chemical Thermodynamic Properties* (National Bureau of Standards, Washington, D.C., 1981).
[23] D. Sanchez-Portal, E. Artacho, and J. M. Soler, Solid State Commun. **95**, 685 (1995).
[24] A. J. Read and R. J. Needs, Phys. Rev. B **44**, 13 071 (1991).
[25] A. L. Dawar and J. C. Joshi, J. Mater. Sci. **19**, 1 (1984).
[26] H. Kageshima and K. Shiraishi, Phys. Rev. B **56**, 14 985 (1997).
[27] D. F. Cox and T. B. Fryberger, Surf. Sci. **227**, L105 (1990).
[28] C. L. Pang, S. A. Haycock, H. Raza, P. W. Murray, G. Thornton, O. Gülseren, R. James, and D. W. Bullett, Phys. Rev. B **58**, 1586 (1998).
[29] S. Gan, Y. Liang, and D. R. Baer, Phys. Rev. B **63**, 121401 (2001).
[30] M. Li, W. Hebenstreit, and U. Diebold, Phys. Rev. B **61**, 4926 (2000).
[31] G.-X. Qian, R. M. Martin, and D. J. Chadi, Phys. Rev. B **38**, 7649 (1988).
[32] J. E. Northrup, Phys. Rev. Lett. **62**, 2487 (1989).
[33] M. Ramamoorthy, R. D. King-Smith, and D. Vanderbilt, Phys. Rev. B **49**, 7709 (1994).
[34] W. C. Mackrodt and P. W. Tasker, J. Am. Ceram. Soc. **72**, 1576 (1989).
[35] Configurational entropy can be estimated from kTln(4) in the case of 1×4 surface domain.
[36] H. Onishi and Y. Iwasawa, Surf. Sci. Lett. **313**, 783 (1994).
[37] K.-O. Ng and D. Vanderbilt, Phys. Rev. B **56**, 10 544 (1997).
[38] R. A. Bennett, Phys. Chem. Commun. **3** (2000).
[39] P. J. Lindan, N. M. Harrison, M. J. Gillan, and J. A. White, Phys. Rev. B **55**, 15 919 (1997).
[40] L. Pauling, *The Nature of the Chemical Bond* (Cornell University Press, Ithaca, 1960).
[41] Cation valence/cation coordination number does not change. This is in agreement with rule that expresses (negative) anion valence of a stable ionic structure as a sum of these quontiets.
[42] C. Noguera, J. Phys.: Condens. Matter **12**, R367 (2000).
[43] J. Terra and D. Guenzburger, Phys. Rev. B **44**, 8584 (1991).
[44] I. Lefebvre, M. A. Szymanski, J. Olivier-Fourcade, and J. C. Jumas, Phys. Rev. B **58**, 1896 (1998).
[45] G. W. Watson, J. Chem. Phys. **114**, 758 (2001).
[46] P. S. Bagus, F. Illas, G. Pacchioni, and F. Parmigiani, J. Electron Spectrosc. Relat. Phenom. **100**, 215 (1999).
[47] D. F. Cox, T. B. Fryberger, and S. Semancik, Phys. Rev. B **38**, 2072 (1988).
[48] R. G. Parr, Philos. Mag. B **69**, 737 (1994).